Proceedings of the
Annual Stability Conference
Structural Stability Research Council
St. Louis, Missouri, April 2-5, 2019

Seismic stability of special concentrically braced frames in a moderate seismic region

Kelley D. M. Grabner[1], Larry A. Fahnestock[2]

Abstract
The special concentrically braced frame (SCBF) system is common in high seismic regions due to its ductile behavior that is enabled by capacity design and detailing requirements. However, SCBFs are used much less frequently in moderate seismic regions, and low-ductility braced frames are more prevalent. To provide a broader perspective on braced frame design and behavior in moderate seismic regions, SCBFs are investigated and compared to the low-ductility systems more typically used in moderate regions, namely the R = 3 CBF and the ordinary concentrically braced frame (OCBF). Nonlinear static and dynamic analyses are used to assess system behavior considering variations in system ductility, frame height, and brace configuration. Global static response is characterized using base shear vs. roof drift response to compare strength, drift capacity and elastic and post-elastic stiffnesses. All CBFs reached comparable levels of base shear in the elastic regions but differed in their post-elastic responses, where the low-ductility CBFs relied on system reserve capacity, and the SCBFs exhibited considerable ductility. The post-elastic stiffness ratios of the R = 3 CBFs and SCBFs were comparable for low-rise frames, whereas taller low-ductility CBFs developed lower post-elastic stiffness ratios than the SCBFs. A FEMA P695 collapse performance assessment is conducted for all CBF model variations. The results are evaluated with two measures: (1) the adjusted collapse margin ratio (ACMR) compared to the required ACMR for 10% probability of collapse and (2) a CBF system weight-normalized performance index (PI). The SCBFs consistently demonstrated lower probabilities of collapse compared to the low-ductility CBFs. Furthermore, the chevron configurations consistently exhibited lower probabilities of collapse than their split-x counterparts for all frames studied. For the SCBFs, the split-x brace configurations had higher PIs than the chevron brace configuration, whereas the low-ductility frames with chevron configuration outperformed the split-x configurations in most cases. For the low-rise frames, the SCBFs had significantly higher PIs than the low-ductility frames, whereas for the taller frames, the PIs were in a narrower range.

1. Background and Previous Research

Special concentrically-braced frames (SCBFs) are high ductility seismic force-resisting systems (SFRSs) that are designed to achieve large inelastic drifts through the primary energy dissipating mechanism of stable yielding and buckling of the braces. The design requirements of SCBFs,

[1] Structural Design Engineer, KPFF Consulting Engineers, <kelley.grabner@kpff.com>
[2] Associate Professor, University of Illinois at Urbana-Champaign, <fhnstck@illinois.edu>

which include ductile detailing and proportioning per the *Seismic Provisions for Structural Steel Buildings* (AISC 2016), ensure the system remains viable and precludes collapse up to large drifts. Recent research on the seismic behavior of SCBFs has contributed to the improved inelastic response of these systems. Roeder et al. (2010) proposed a balanced design procedure (BDP) that maximizes the drift capacity of the frame by balancing the inelastic behavior of the braces in buckling and yielding with desired ductile yield mechanisms in other components (e.g. gusset plate yielding). Gusset plates designed with the BDP were experimentally tested in full-scale frames (Roeder et al. 2011), and the results showed improved drift capacity compared to the conventional gusset plate in that the new gusset plates permitted larger out-of-plane deformations of the braces and greater plate yielding. These favorable inelastic mechanisms enabled the HSS braces to provide significant ductility, reaching maximum story drifts of 2% before brace fracture. Recent research on SCBFs has also included numerical simulations of complete SCBF systems for the assessment of seismic performance (Hsiao et al., 2013).

Prior to 1988, CBFs in high seismic regions did not have the prescriptive capacity design or ductility requirements that are present in the current AISC *Seismic Provisions* for SCBFs, so they are regarded as nonductile CBFs. Sen et al. (2016) experimentally tested four two-story chevron braced frame specimens to investigate the effect of the pre-1988 design deficiencies of nonductile CBFs, including nonductile braces, nonductile connections, and low axial-flexural capacity beams. The brace sections, beam-to-column connections, and brace-to-gusset welds that were noncompliant with the current *Provisions* exhibited a detrimental impact on the frame behavior, contributing to the nonductile response. However, the weak beams (with demand-to-capacity ratios up to 2.5) were shown to produce a favorable yielding beam mechanism that had minimal detriment on the overall inelastic drift capacity and the lateral resistance of the frame. This result suggests that the yielding beam mechanism may not be a deficiency and that the current capacity design requirements for SCBFs which result in strong and stiff beams in chevron configurations could be revisited.

While recent research initiatives have improved the design requirements and resulting behavior of SCBFs, these systems are typically only designed in high seismic regions, and they are not frequently designed where a lower ductility CBF is permitted because of the increased system cost and design effort associated with SCBFs. Low-ductility CBFs are more common in low and moderate seismic regions. Low-ductility CBFs are permitted to be designed at a reduced seismic force level, but they do not have the same rigorous detailing or proportioning requirements as SCBFs. The OCBF has brace ductility requirements and partial capacity design requirements, whereas the $R = 3$ CBF has no additional seismic design requirements. The seismic response of low-ductility CBFs relies on reserve capacity, or secondary stiffness and strength following initial nonductile limit states. Recent research has investigated the sources of reserve capacity in low-ductility CBFs with full-scale experimental testing and numerical simulations (Hines et al. 2009; Bradley 2016; Sizemore 2017). In numerical simulations of a three-story $R = 3$ chevron CBF, Sizemore (2017) observed a beneficial long-link eccentrically-braced frame (EBF) mechanism form in the first story when the brace-to-gusset weld fractured, and the flexural reserve strength of the beam was engaged. A numerical simulation of a three-story OCBF chevron exhibited the same initial brace-to-gusset weld fracture as the $R = 3$ CBF, but a subsequent brace weld fracture occurred at the one remaining brace in the first story. This succession of limit states produced a soft story mechanism and led to frame collapse. The OCBF chevron was designed according to partial capacity design requirements, which produced a very stiff beam; however, the OCBFs do not have additional proportioning or detailing requirements, so the welds and connections can be suscpetible to fracture, which was the case in the previous example. The research identifying and quantifying low-ductility reserve capacity provides a basis for discussing potential improvements SCBFs can provide to moderate seismic applications.

This brief review of the research characterizing SCBF behavior and low-ductility CBF behavior highlights the complexities of inelastic CBF seismic response. When capacity design requirements and ductile detailing are present in the design of the system, as in SCBFs, the resulting behavior is typically characterized by large inelastic drift capacity due to stable brace buckling and yielding. The behavior of low-ductility CBFs is characterized by an initial brittle limit states and significant loss of strength and stiffness followed by a region of reserve capacity. The sources of reserve capacity are inherent to the system, and they are not guaranteed in the design process, thus they are challenging to predict or rely on for structural stability. This research investigates the seismic stability of SCBFs designed for moderate seismic regions through numerical simulations of a suite of SCBFs that includes variations in brace configuration, frame height, and gravity column contribution.

2. SCBF Numerical Model

A suite of SCBFs was designed according to the AISC *Seismic Provision* for the same prototype building used in previous analyses of low-ductility braced frame systems (Bradley 2016, Sizemore 2017). The design suite considered frames of three, six, and nine stories and braces configured as two-story x (split-x) and chevron. The naming convention for these designs that is used throughout the paper is as follows [CBF Type]-[SX or CH]-[3,6, or 9]. For example, SCBF-SX-6 corresponds to the six-story split-x SCBF.

The low-ductility CBF model in OpenSees developed by Sizemore (2017) was adapted to create a numerical SCBF model that captures the pertinent nonlinear structural behavior expected of the high ductility system, including brace buckling and yielding, gusset plate yielding, and cyclic degradation of structural members. The limit state of weld fracture incorporated in the low-ductility CBF model was not used in the SCBF model since the capacity design and detailing of the SCBFs preclude that limit state. The nonlinear analyses of low-ductility CBFs from Sizemore (2017) were reproduced and results are included here for comparison. The model incorporated the effects of numerous design and analysis variations on frame stability, including: chevron or split-x brace configurations; three, six and nine story frames; and gravity columns that are either continuous over all stories or pinned at each story. The results of these numerical investigations are used for low-ductility versus high-ductility CBF comparison, considering the influences of brace configuration and story height.

The SCBF model represented braces with distributed plasticity elements to capture the effects of axial-flexural interaction and imperfections, and the braces were wrapped in a fatigue material to capture the effects of cyclic degradation. Beams and columns were modeled with concentrated plasticity elements to simplify the nonlinear model. The concentrated plasticity elements enabled the direct modeling of cyclic degradation on the nonlinear moment-rotation relationship defined for each frame member. The gusset plates were designed with the $8t_p$ elliptical clearance of the BDP and were modeled with nonlinear springs representing the gusset plate yielding behavior.

Since a two-dimensional frame model was used for computational efficiency, brace buckling was modeled in plane and the gusset plate nonlinear spring was also oriented for in-plane behavior.

Nonlinear static and dynamic analyses were conducted for use in a collapse performance assessment based on the FEMA P695 framework (2009). The nonlinear static, or pushover, analyses are useful in characterizing system behavior, including the progression of limit states and their effect on frame stability. The nonlinear static analyses also enable the definition and comparison of changes in stiffness and strength with increasing drift demand for the CBF models. The destabilizing P-Δ effect was captured by the direct application of gravity load on the gravity columns of the model at a magnitude of 1.0D + 0.2L, consistent with the recommendations of FEMA P695. Nonlinear response history analyses were conducted with a suite of 15 ground motions developed for Boston, Massachusetts (Hines et al., 2009; Hines et al. 2011). As a suite, these ground motions were scaled to the MCE to capture response variations across a larger range of periods consistent with the behavior of typical east coast low-ductility CBFs. The incremental dynamic analysis (IDA) procedure was employed wherein the suite of CBF models were subjected to each ground motion at increasing scale factors until collapse occurs. The collapse criteria selected for the IDAs was a maximum story drift of 5%, representing the drift beyond which the beam-column-gusset connections in an SCBF lose considerable stiffness and no longer ensure rigid frame action. Additionally, this story drift maintains consistency with recent IDAs of SCBFs (Hsiao et al. 2013). The IDA produces collapse fragilities from which the collapse margin ratio and probability of collapse for each frame can be ascertained and compared across the CBF model variations for different systems.

3. Nonlinear Static Characterization

3.1. SCBF Analyses

Nonlinear static (pushover) analyses are conducted with the CBF models to assess the seismic stability of the structures. Pushover analyses provide insight into the stiffness and strength of the systems with increasing drift demands. The effect of gravity loading is included in the models to determine the influence of destabilizing P-Δ effects on the systems. The results of the pushover analyses are presented as a set of response variables, specifically base shear, roof drift and stiffness defined for various domains of the system response. The response variables are defined in Table 1 and presented graphically on a representative pushover curve in Fig. 1.

The base shear and roof drift response values are obtained from the pushover curves. The stiffness of the system changes throughout the pushover analysis, beginning with a region of elastic behavior followed by subsequent inelastic regions that transition from positive stiffness to negative stiffness, which leads to collapse of the system. It is useful to quantify the stiffnesses beyond the elastic region to evaluate and compare the seismic stability of the systems. To characterize the important features of nonlinear behavior, secant stiffness is calculated for three post-elastic regions: (1) elastic limit to $V_{b,max}$, (2) $V_{b,max}$ to $0.8V_{b,max}$, and (3) $0.8V_{b,max}$ to collapse (i.e. zero base shear). These three quantities are all generically termed secondary stiffnesses, and they characterize the static collapse response of a system. The ratio of the secondary stiffness to the elastic stiffness of each system is computed to make comparisons across the frame variations. A summary of base shear and roof drift, and stiffness response variables is provided in Tables 2 and 3, respectively.

Table 1. Descriptions of Pushover Response Variables

Variable	Description
Elastic base shear ($V_{b,elastic}$)	Base shear at the end of the elastic region.
Roof drift at $V_{b,elastic}$	Roof drift (%) at the end of the elastic region.
Maximum base shear ($V_{b,max}$)	Maximum base shear capacity of the system.
Roof drift at $V_{b,max}$	Roof drift (%) at the maximum base shear.
Ultimate displacement (δ_u)	FEMA P695 defines ultimate displacement as the displacement corresponding to 80% of the maximum base shear.
Base shear at δ_u	80% of the maximum base shear.
Roof drift at δ_u	Roof drift (%) at 80% of the maximum base shear.
Collapse drift (δ_c)	Drift at zero base shear.
Initial stiffness (K_1)	Elastic stiffness of the frame.
Secondary stiffnesses (K_2, K_3, K_4)	Secondary secant stiffnesses are calculated over three regions of the response beyond the elastic region.

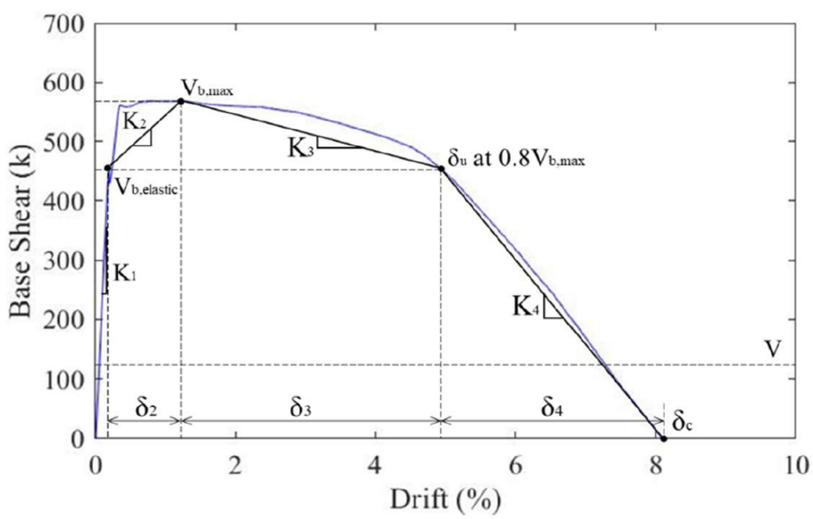

Figure 1. SCBF-SX-3 Pushover curve response variables

The SCBF pushover responses all exhibited an initial elastic response followed by softening of the structure and strength loss until collapse. This strength degradation is characteristic of the P-Δ effect of the gravity loads acting on the lateral displacements of the structure, which generates a destabilizing overturning moment. The effect of pinned versus continuous gravity column modeling had minimal contribution to the maximum base shear capacity and corresponding roof drift of the systems. That is, $V_{b,max}$ was reduced by an average of only 3% and the roof drift at $V_{b,max}$ decreased by an average of 0.2% drift when the gravity columns were pinned. Removing the gravity column contribution to the lateral resistance of the CBFs did have a noticeable effect of reducing the overall drift capacity of the systems by 16%. The elastic and secondary stiffnesses indicate that the initial elastic response of the system does not engage the gravity columns, but the first region of negative secondary stiffness (K_3) increases in magnitude with the pinned gravity columns, eventually producing a reduced drift capacity for the system.

Table 2. Pushover response variables: base shear and roof drift

Frame ID	$V_{b,elastic}$		$V_{b,max}$		δ_u ($0.8V_{b,max}$)		Collapse
	Base Shear (k)	Roof Drift (%)	Base Shear (k)	Roof Drift (%)	Base Shear (k)	Roof Drift (%)	Roof Drift (%)
SCBF-SX-3-CONT	461	0.19	568	1.2	454	4.9	8.0
SCBF-SX-3-PIN	461	0.19	560	0.3	448	2.8	6.1
SCBF-CH-3-CONT	511	0.19	586	0.7	469	4.7	8.5
SCBF-CH-3-PIN	511	0.19	567	0.5	454	3.4	8.4
SCBF-SX-6-CONT	261	0.24	346	1.0	277	5.4	10.0
SCBF-SX-6-PIN	261	0.24	340	1.0	272	3.8	9.1
SCBF-CH-6-CONT	268	0.15	391	1.1	313	2.8	9.9
SCBF-CH-6-PIN	268	0.15	374	0.9	300	2.7	7.1
SCBF-SX-9-CONT	403	0.47	448	0.6	359	2.1	6.0
SCBF-SX-9-PIN	403	0.47	441	0.6	353	1.6	4.2
SCBF-CH-9-CONT	180	0.16	359	0.7	387	1.5	3.0
SCBF-CH-9-PIN	180	0.16	346	0.7	377	1.5	2.8

Table 3. Pushover response variables: stiffness

Frame ID	Region 1		Region 2		Region 3		Region 4	
	K_1 (k/in)	δ_1 (%)	K_2/K_1 (%)	δ_2 (%)	K_3/K_1 (%)	δ_3 (%)	K_4/K_1 (%)	δ_4 (%)
SCBF-SX-3-CONT	454	0.2	4.2	1.1	-1.3	3.7	-6.0	3.1
SCBF-SX-3-PIN	454	0.2	26.7	0.2	-1.8	2.5	-5.6	3.3
SCBF-CH-3-CONT	506	0.2	5.7	0.5	-1.1	4.0	-4.5	3.8
SCBF-CH-3-PIN	506	0.2	6.1	0.3	-1.4	2.9	-3.3	5.0
SCBF-SX-6-CONT	98.9	0.2	11.2	0.7	-1.5	4.4	-5.6	4.6
SCBF-SX-6-PIN	98.9	0.2	9.4	0.8	-2.3	2.8	-4.8	5.3
SCBF-CH-6-CONT	170	0.1	7.3	0.9	-2.4	1.8	-2.4	7.1
SCBF-CH-6-PIN	170	0.1	7.9	0.7	-2.3	1.8	-3.7	4.4
SCBF-SX-9-CONT	52.8	0.5	33.2	0.2	-7.4	1.4	-10.6	4.0
SCBF-SX-9-PIN	52.8	0.5	34.0	0.1	-9.9	1.0	-16.0	2.6
SCBF-CH-9-CONT	70.0	0.2	31.4	0.5	-7.3	0.9	-17.0	1.5
SCBF-CH-9-PIN	70.0	0.2	25.9	0.6	-7.5	0.8	-19.8	1.2

Note: δ_1 to δ_4 describe the drift range over which each stiffness ratio is defined, not a coordinate of drift.

The chevron frames exhibited higher elastic stiffnesses than their comparable split-x frames as expected due to the stronger and stiffer beams required in the chevron configuration to satisfy the unbalanced force requirement for chevron SCBFs. Despite the higher elastic stiffnesses, the chevron braced frames did not consistently achieve a higher base shear capacity, as seen in the case of the 9 story SCBFs. In general, the behavior of the chevron SCBFs is characterized by tension brace yielding and compression brace buckling in the stories that exhibit inelasticity. This contrasts with the response of the split-x frames that do not typically achieve both yielding and buckling in a single story because the connection of the braces across the two-story x distributes the inelasticity across multiple stories.

K_2/K_1 describes the increase in system strength between the end of the elastic region and the point of maximum base shear. The associated drift range, δ_2, is an important quantity to consider alongside the stiffness ratio. A high ratio alone does not indicate preferred frame response, but the combination of a larger drift range, δ_2, and a moderate K_2/K_1 ratio was generally seen for frames that maintained base shear capacity at large drift demands. (For example, SCBF-SX-3-PIN had K_2/K_1 = 26.7% over a drift range δ_2 = 0.2%. SCBF-SX-3-CONT frame had K_2/K_1 = 4.2% over a drift range δ_2 = 1.1%. The CONT frame reached a higher maximum base shear at a larger roof drift, and ultimately achieved a larger drift capacity at collapse than the PIN frame.) K_3/K_1 describes the progression of system strength from $V_{b,max}$ to $0.8V_{b,max}$, the ultimate roof displacement as defined in FEMA P695. This secondary stiffness ratio was negative for all frames and is related most to the frame height. This indicated that the destabilizing effect of P-Δ drives the system response past the point of $V_{b,max}$. For taller frames, the K_3/K_1 ratios become more negative since the P-Δ effect is exacerbated in taller frames. K_4/K_1 describes the destabilizing stiffness of the system until collapse, and no clear trend was observed from this parameter.

3.2 Low and High Ductility CBF Comparison

The response of low-ductility CBFs that are commonly used in moderate seismic regions is characteristically different than the response of high-ductility SCBFs. The low-ductility frames suffer an initial brittle limit state that produces a large drop in strength, after which there is a region of post-elastic positive stiffness until a secondary system peak strength, termed reserve capacity. This characteristic shape is schematically shown in Fig. 2.

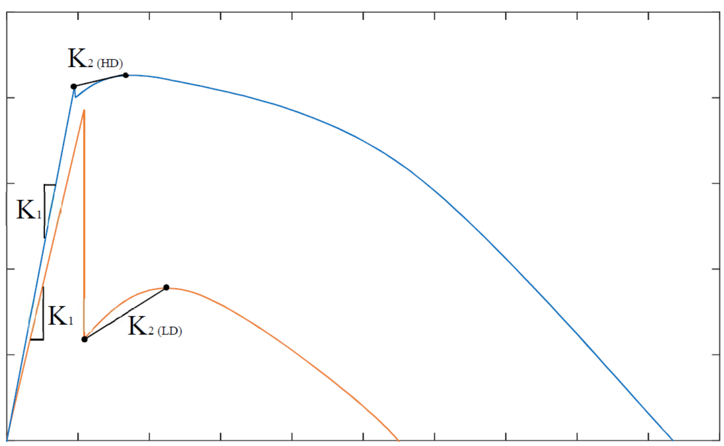

Figure 2. Low-ductility versus high-ductility CBF pushover response: schematically showing the K_1 elastic stiffness, and K_2 secondary stiffness (HD) / post-elastic stiffness (LD)

The R = 3 CBF, OCBF, and SCBF are compared on the basis of their stiffness ratios since these are the most analogous paraments describing the nonlinear behavior of each system. The secondary stiffness values of the SCBFs are computed as illustrated in the above figure and consistent with the definitions in Section 3.1. The most comparable response variable to the secondary stiffness for the R = 3 CBF and OCBF is the post-elastic stiffness computed as illustrated in the Fig. 2. This stiffness ratio describes the rate at which the system gains reserve capacity following the initial nonductile limit states. The secondary and post-elastic stiffnesses are labeled K_2 and the stiffness ratios for each frame are presented in Tables 4, 5 and 6.

Comparing the three system types, the elastic stiffnesses of all frames for a given story height are similar to one another. The R = 3 CBFs and the SCBFs exhibit the closest elastic stiffnesses, and the OCBF consistently has a higher elastic stiffness than the SCBF. The K_2/K_1 terms for the low-ductility CBFs at times exceed the SCBF (e.g. R = 3 SX-6 and OCBF-CH-6). Although these terms differ in their definitions between the low-ductility and high-ductility CBFs, this observation indicates that there is a significant post-elastic response available to low-ductility frames. However, the sources of reserve capacity for low-ductility systems vary and are less predictable in nature than the stable inelastic response exhibited by the SCBFs.

Table 4. R = 3 CBF elastic stiffness and post-yield stiffness ratio

Frame ID	K_1 (k/in)	K_2/K_1 (%)
R3-SX-3	427.8	4.2
R3-CH-3	437.9	6.3
R3-SX-6	134.0	38.2
R3-CH-6	154.6	5.3
R3-SX-9	76.1	14.1
R3-CH-9	86.0	17.2

Table 5. OCBF elastic stiffness and post-yield stiffness ratio

Frame ID	K_1 (k/in)	K_2/K_1 (%)
OCBF-SX-3	525.2	0.6
OCBF-CH-3	765.1	2
OCBF-SX-6	133.7	6.2
OCBF-CH-6	249.2	8.7
OCBF-SX-9	82.8	9.2
OCBF-CH-9	125.0	18.1

Table 6. SCBF elastic stiffness and post-yield stiffness ratio

Frame ID	K_1 (k/in)	K_2/K_1 (%)
SCBF-SX-3	453.7	4.2
SCBF-CH-3	506.2	5.7
SCBF-SX-6	98.9	11.2
SCBF-CH-6	170.2	7.3
SCBF-SX-9	52.8	33.2
SCBF-CH-9	70.0	31.4

4. Seismic Performance Assessment

4.1 SCBF Performance Assessment

Nonlinear dynamic analyses were conducted as a key part of the seismic performance assessment of SCBFs to gain insight beyond what could be gleaned from the static analyses, namely the response of the structure including the effects of structural degradation from the numerous cycles of loading characteristic of realistic earthquake demands. FEMA P695 presents a methodology for conducting dynamic analyses as a part of the comprehensive collapse performance assessment of structural systems. Incremental dynamic analyses are used to determine the median collapse intensity and collapse margin ratio (CMR) for each system. The median collapse intensity is the spectral acceleration at which half of the ground motion records produce collapse. FEMA P695 defines the CMR as the ratio of the median collapse intensity to the maximum considered earthquake (MCE) acceleration at the fundamental period. In the case of the Hines et al. (2009) ground motion set that was used in this research, a scale factor equal to unity corresponded to the MCE intensity. For this reason, the collapse margin ratio is equivalent to the scale factor at median collapse. The criteria used to determine collapse was a maximum story drift of 5%, consistent with the criteria used by Hsiao et al. (2009) in incremental dynamic analysis of SCBFs. Furthermore, this criteria represents the story drift at which the beam-column-gusset connections would lose considerable stiffness and connection integrity. Since this limit state was not captured by the model directly, it is appropriate to establish 5% story drift as the collapse criteria. The above definitions were employed when processing the IDA data to construct collapse fragility curves. The collapse fragility is a relationship between the ground motion intensity and the probability of collapse. The main objective of this section is to present and discuss the data obtained from the final collapse fragility curves for assessing the performance of the SCBFs in this study. Fig. 3 illustrates representative IDA results.

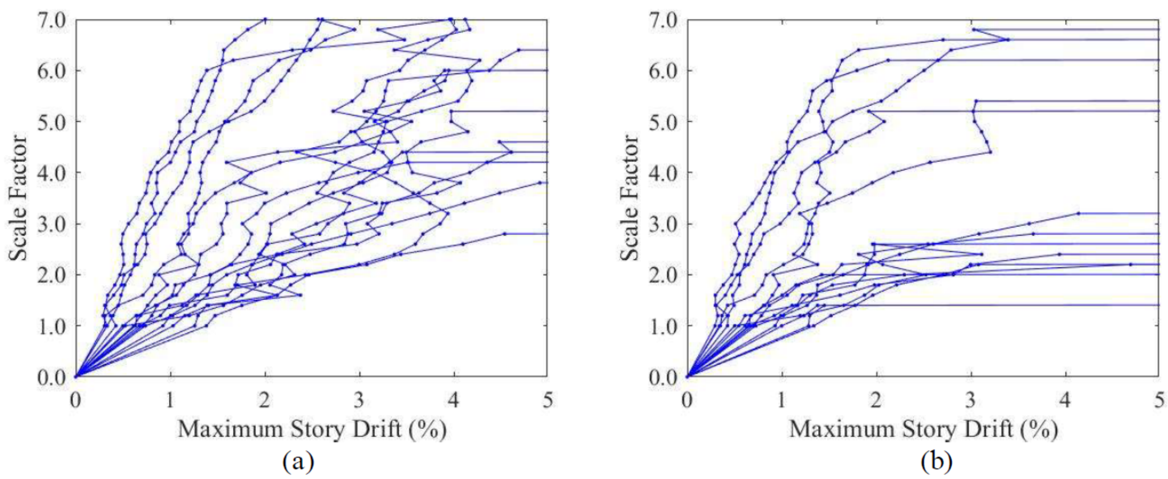

Figure 3. Incremental dynamic analysis ground motions suite results: (a) SCBF-CH-3-CONT (b) SCBF-CH-3-PIN

The IDAs above exhibit “weaving’ where the curve irregularly approaches a collapse scale factor. This phenomenon was additionally observed in the evaluation of low-ductility CBFs (Hines et al. 2009; Sizemore 2017; Sizemore et al. 2019). Here it was concluded that the dependence of low-ductility systems on the sequence of limit states contributed to the IDA weaving. This characteristic of the IDA is not as common for high-ductility systems; however, the scaled ground motion set had a wide range of frequency content that contributed to the variability of the excitation and response of the SCBFs. Fig. 3a presents an example where collapse was not achieved for all 15 of the ground motions. Hsiao et al. (2013) similarly observed SCBFs not achieving collapse at large scale factors for a minority of the ground motions in the IDA set, but this occurrence is not a limitation in the FEMA P695 procedure since it only requires the median collapse intensity to be determined from the IDAs. The median collapse intensity is then used to determine the CMR, which is used along with the total collapse uncertainty, or the dispersion of the collapse predictions (β_{TOT}), to define probability of collapse. Rather than computing β_{TOT} from the dispersion of the dynamic analysis results, the total collapse uncertainty is calculated from four sources: (1) record-to-record uncertainty, (2) design requirements uncertainty, (3) test data uncertainty, and (4) modeling uncertainty. The total collapse uncertainty is calculated as:

$$\beta_{TOT} = \sqrt{\beta_{RTR}^2 + \beta_{DR}^2 + \beta_{TD}^2 + \beta_{MDL}^2} \tag{1}$$

Table 7 summarizes the values of each contribution to uncertainty and the total collapse uncertainty. As a comparison to other systems analyzed for moderate seismic regions, the total collapse uncertainty was 0.65 for OCBFs and 0.75 for R = 3 CBFs (Sizemore 2017).

Table 7. Summary of uncertainties

Uncertainty	Variable	Value	Explanation
Record-to-record uncertainty	β_{RTR}	0.4	Fixed value suggested by FEMA P695
Design requirements uncertainty	β_{DR}	0.2	Design includes reasonable safeguards against unanticipated failure modes
Test data uncertainty	β_{TD}	0.35	Foundational SCBF test data available, but not specific to SCBFs in moderate seismic regions
Modeling uncertainty	β_{MDL}	0.2	Model captures essential realistic structural behavior at the element and global levels
Total collapse uncertainty	$\boldsymbol{\beta_{TOT}}$	**0.6**	

Representative collapse fragility curves constructed from the previously defined variables are shown in Fig. 4. The probability of collapse at the MCE, $p(C)_{MCE}$ is the ordinate of the fragility curve at a scale factor of unity. The CMR corresponds to the median collapse intensity, as defined before, and it can be seen as the point at 50% probability on the fragility curve. The adjusted collapse margin ratio, ACMR, is defined as ACMR = SSF*CMR. In this research CMR is equal to ACMR since period-based ductility is taken as 1.0 and the spectral shape factor, SSF, is thus also 1.0 (Sorabella 2006; FEMA 2009). In lieu of presenting the eight individual SCBF collapse fragility curves, Table 8 presents a summary of the pertinent data gathered from these plots that is used in the collapse performance assessment.

In the FEMA P695 framework, probability of collapse at the MCE, $p(C)_{MCE}$, less than or equal to 0.1 on average across a performance group is the basic acceptance criterion. Although FEMA P695 allows individual cases within a performance group to only satisfy $p(C)_{MCE} \leq 0.2$, $p(C)_{MCE} \leq 0.1$ is used uniformly as the acceptance criterion in this research. The acceptance criterion $p(C)_{MCE} \leq 0.1$ can also be stated as ACMR $\geq$ $ACMR_{10\%}$. The final column of Table 8 presents the results of this performance evaluation for each SCBF model, and all of the SCBFs designed for moderate seismic regions passed. Even though all model variations had satisfactory performance, the models that included continuous gravity columns performed markedly better than those with pinned gravity columns. On average, the ACMR increased by 35% when the gravity columns were modeled as continuous compared to pinned. This indicates that the gravity column flexural capacities are engaged in the overall lateral resistance of the system. The beneficial effect of gravity columns was larger for the three-story frames than for the six-story frames. This suggests that the shorter frames were more prone to developing story mechanisms that engaged gravity column flexure. In general, the chevron configuration performed better than the split-x configurations for both the three and six-story SCBFs, with higher ACMR (lower $p(C)_{MCE}$).

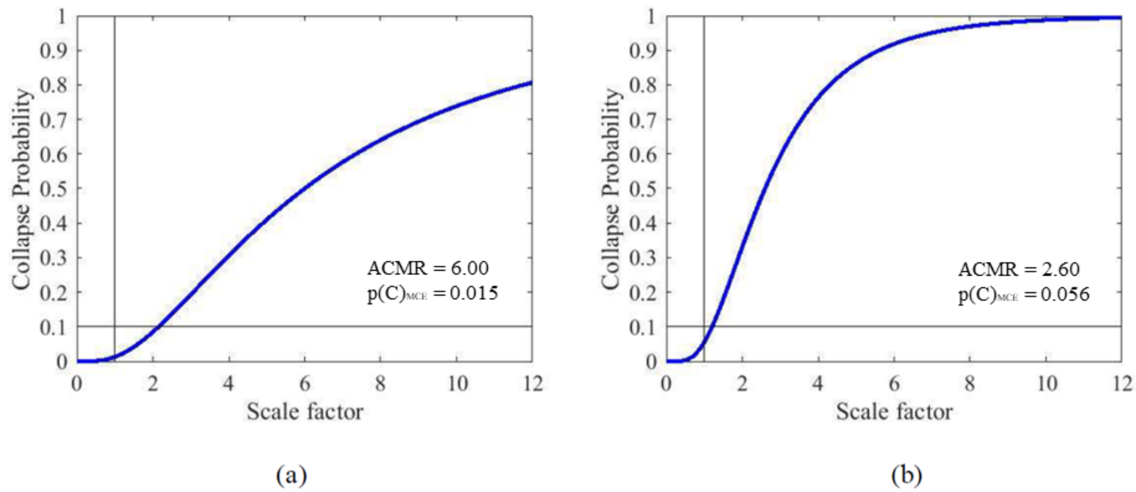

Figure 4. Collapse fragility curves: (a) SCBF-CH-3-CONT (b) SCBF-CH-3-PIN

Table 8. Collapse performance evaluation of SCBFs

Frame ID	ACMR	Acceptance Criteria	
		$ACMR_{10\%}$	Pass/Fail
SCBF-SX-3-CONT	5	2.16	Pass
SCBF-SX-3-PIN	4	2.16	Pass
SCBF-CH-3-CONT	6	2.16	Pass
SCBF-CH-3-PIN	2.6	2.16	Pass
SCBF-SX-6-CONT	3.8	2.16	Pass
SCBF-SX-6-PIN	3.2	2.16	Pass
SCBF-CH-6-CONT	5.2	2.16	Pass
SCBF-CH-6-PIN	5	2.16	Pass

4.2 Low and High Ductility CBF Performance Comparison

An additional objective of this performance evaluation is to compare the high-ductility SCBFs with the low-ductility R = 3 CBFs and OCBFs typical of moderate seismic regions. In a prior study (Sizemore 2017; Sizemore et al. 2019), the collapse criteria used in the analysis for low-ductility CBFs was when any story reached a drift ratio of 10%, which is different than the criteria defined for SCBFs. However, the research noted that once 3% story drift was recorded in the low-ductility CBF analyses, it took few additional time steps before the story drift increased to the 10% criteria. For this reason, there is no appreciable difference in the formulation of the collapse criteria for both system types, and a direct comparison of the collapse probabilities and ACMRs is still appropriate. The collapse performance assessment findings from Sizemore

(2017) are referenced in Tables 9 and 10 for the three and six-story frames, respectively, in addition to the SCBFs.

Table 9. Collapse performance evaluation comparison of three-story low and high-ductility CBFs

Frame ID	ACMR	Acceptance Criteria			Weight-Normalized Performance	
		$ACMR_{10\%}$	$p(C)_{MCE}$	Pass/Fail	W_{CBF} (tons)	PI
SCBF-SX-3	5.00	2.16	0.025	Pass	9.1	0.254
SCBF-CH-3	6.00	2.16	0.015	Pass	13.3	0.209
OCBF-SX-3	1.24	2.30	0.370	Fail	6.9	0.078
OCBF-CH-3	3.20	2.30	0.040	Pass	9.8	0.142
R3-SX-3	1.07	2.61	0.460	Fail	5.9	0.069
R3-CH-3	2.17	2.61	0.150	Fail	5.9	0.141

Table 10. Collapse performance evaluation comparison of six-story low and high-ductility CBFs

Frame ID	ACMR	Acceptance Criteria			Weight-Normalized Performance	
		$ACMR_{10\%}$	$p(C)_{MCE}$	Pass/Fail	W_{CBF} (tons)	PI
SCBF-SX-6	3.80	2.16	0.050	Pass	19.0	0.093
SCBF-CH-6	3.20	2.16	0.022	Pass	26.4	0.091
OCBF-SX-6	2.59	2.30	0.070	Pass	12.6	0.089
OCBF-CH-6	3.32	2.30	0.030	Pass	18.4	0.078
R3-SX-6	2.06	2.61	0.170	Fail	11.8	0.067
R3-CH-6	2.53	2.61	0.110	Fail	12.0	0.081

From the above comparison, it is clear the SCBFs outperformed the R = 3 CBFs in both the three-story and six-story frames. These systems represent opposite ends of the spectrum in terms of their design requirements ensuring ductile seismic response, considering that the design of the R = 3 CBF was governed by AISC 360 only, even though the system was designed to a reduced seismic force level. The differences in collapse performance between the SCBF and the OCBF are more nuanced. At the three-story height, the OCBF-SX failed the performance evaluation while the SCBF passed, $p(C)_{MCE}$ are significantly different between system types . At the six-story height, the SCBFs and OCBFs both passed the performance evaluation and $p(C)_{MCE}$ for the OCBFs are approximately 40% greater than for the corresponding SCBFs. Thus, with increased story heights, there may not be as significant of an advantage in selecting a higher ductility system like the SCBF when the OCBF is also permitted. For all CBF types, the chevron configuration consistently performed better than the split-x frames, which contrasts the findings of the nonlinear static analyses. The nonlinear static analysis results showed that the split-x frames had higher drift at collapse for the majority of cases. However, the dynamic analyses included critical aspects of the structure's seismic response that were not captured in the pushovers, specifically the effect of strength degradation and the excitation of higher mode responses. The split-x frames were more susceptible to undesirable performance with the addition of these effects in the dynamic analyses.

To further compare the collapse performance evaluation results, a weight normalized performance index, PI, is introduced as a simplistic metric to combine seismic performance and structural efficiency. The performance index is defined as, PI = $(ACMR/ACMR_{10\%})/W_{CBF}$, where W_{CBF} is the weight in US tons. Although this ratio does not have a scientific meaning (and it depends on the units used for weight), it does provide a measure that combines collapse stability and structural weight, and thus is useful for relative comparisons within a specific research study between different SFRSs designed for the same building. A higher PI corresponds to better performance. The PIs for the three and six-story frames are included in Tables 9 and 10, respectively.

The chevron and split-x SCBFs consistently performed better than the OCBF and R = 3 systems at both the three-story and six-story heights according to the PI. The two different configurations of SCBF demonstrated similar PI, as the heavier chevron configurations exhibit increased collapse resistance. However, for the cases studied, the split-x SCBF has slightly higher PI than the chevron SCBF. For the low-ductility systems, the chevron configurations have more favorable PI than the corresponding split-x configurations in the majority of the cases. For the three-story frames, there is a significant gap in PI between the SCBFs and the low-ductility systems. For the six-story frames, the PI trend decreases from SCBF to OCBF to R = 3, but the range of PI is narrower.

5. Summary and Conclusions

The evaluation of SCBF seismic performance in this paper provides a high-ductility perspective to compare to the design and behavior of CBFs in moderate seismic regions. The nonlinear static analyses produced response variables quantifying the maximum base shear capacity and roof drift, the elastic stiffness, and the secondary stiffnesses for each system. A comparison of the relative post-elastic stiffnesses of the SCBFs and low-ductility CBFs provides insight into the ability of the systems to develop strength and positive stiffness beyond the elastic region. In general the low-ductility systems relied heavily on the flexural stiffness of the gravity columns to provide this positive post-elastic stiffness to achieve reserve capacity. The low-ductility CBFs demonstrated inelasticity in elements other than the braces, such as beam yielding before demands concentrated in a story, forming a mechanism. The structural behavior experienced by the SCBFs differed in that they engaged tensile brace yielding and compression brace buckling to dissipate seismic energy, and beyond the inelastic capacity of the braces, the SCBFs engaged flexural strength of the columns prior to collapse. The SCBF pushover curves were characterized by a region of elastic response followed by secondary stiffness regions that gradually became more negative until P-Δ effects drove the collapse of the system. The destabilizing effects of P-Δ were exacerbated in the taller SCBF frames.

The seismic performance of the SCBFs was further evaluated by conducting incremental dynamic analyses (IDAs) for use in the collapse assessment described in FEMA P695. The results of the collapse performance assessment of the three-story and six-story SCBFs were compared to the previous seismic performance evaluation of low-ductility braced frames (Sizemore 2017; Sizemore et al. 2019). A weight-normalized performance index, PI, was used to compare system performance and roughly judge the effectiveness of increased system weight. The SCBFs outperformed the low-ductility CBFs according to the PIs and the probabilities of collapse. The PIs indicated that the weight-normalized performance of the SCBFs was not highly dependent on brace configuration. That is, the PIs of SCBFs in the chevron or split-x brace configuration were relatively close, for each frame height variation. Per the FEMA P695 performance criteria, the chevron SCBFs produced lower probabilities of collapse, but according to the PIs, which adjusted for the substantially higher system weights of chevron frames (that resulted from capacity design requirements), the split-x counterparts narrowly outperformed the chevron frames. For the majority of the low-ductility systems, the chevron brace configuration identified as having the lower probability of collapse also had the higher PI. Finally, for the low-rise frames, the SCBFs had significantly higher PIs than the low-ductility frames, whereas for the taller frames, the PIs were in a narrower range. This indicates that for taller buildings in moderate seismic regions where low-ductility CBFs are permitted, there may not be as significant a performance advantage in selecting a higher ductility system like the SCBF.

Acknowledgements

The first author was partially funded by a Carver Fellowship from the College of Engineering at the University of Illinois at Urbana-Champaign. This work used the Extreme Science and Engineering Discovery Environment (XSEDE), which is supported by National Science Foundation Grant No. ACI-1548562. The opinions, findings, and conclusions in this paper are those of the authors and do not necessarily reflect the views of those acknowledged here.

References

AISC. (2016). "Seismic provisions for structural steel buildings." ANSI/AISC 341-16, *American Institute of Steel Construction*. Chicago, IL.

Bradley, C. (2016). "Experimental investigation of post-elastic failure mechanisms in low-ductility braced frames and the implications for collapse performance." *Master's Thesis.* Tufts University. Medford, MA.

Bradley, C. R., Fahnestock, L. A., Hines, E. M., Sizemore, J. G. (2017). "Full-scale cyclic testing of low ductility concentrically braced frames." *Journal of Structural Engineering*. 143(6).

Federal Emergency Management Agency. (2009). "Quantification of Building Seismic Performance Factors." FEMA P695. Applied Technology Council. Redwood City, CA.

Grabner, K. D. M. (2018). "Performance Assessment of Special Concentrically-Braced Frames in Moderate Seismic Regions." *Master's Thesis.* The University of Illinois at Urbana-Champaign.

Hines, E. M., Appel, M.E., Cheever, P. J. (2009). "Collapse Performance of Low-Ductility Chevron Braced Steel Frames in Moderate Seismic Regions." *Engineering Journal*, American Institute of Steel Construction. 46: 149-180.

Hines, E. M. Baise, L. G., Swift, S. S. (2011). "Ground-motion suite selection for Eastern North America." *Journal of Structural Engineering.* 137(3): 358-366.

Hsiao, P-C, Lehman, D.E., Roeder, C.W. (2013). "Evaluation of response modification coefficient and collapse potential of SCBFs." *Earthquake Engineering and Structural Dynamics*. 42(10): 1547-1564

Roeder, C. W., Lehman, D. E. Clark, K., Powell, J., Yoo, J., Tsai, K., Lin, C., Wei, C. (2010). "Influence of gusset plate connections and braces on the seismic performance of the X-braced frames." *Earthquake Engineering and Structural Dynamics*. 40: 355-374.

Roeder, C. W. Lumpkin, E. J., Lehman, D. E. (2011). "A balanced design procedure for special concentrically braced frame connections." *Journal of Construction Steel Research*.

Sen, A. D., Roeder, C. W., Berman, J. W., Lehman, D. E., Li, C. H., Wu, A. C., Tsai, K. C. (2016). "Experimental Investigation of Chevron Concentrically Braced Frames with Yielding Beams." *Journal of Structural Engineering*.

Sizemore, J.G. (2017). "Inelastic Behavior and Seismic Collapse Prevention Performance of Low-Ductility Steel Braced Frames." *Doctoral Dissertation.* The University of Illinois at Urbana-Champaign.

Sizemore, J., Fahnestock, L., Hines, E., and Bradley, C. (2017). "Parametric Study of Low-Ductility Concentrically-Braced Frames under Cyclic Static Loading." *Journal of Structural Engineering*. 143(6).

Sizemore, J., Fahnestock, L., and Hines, E. (2019). "Seismic Performance Assessment of Low-Ductility Concentrically Braced Frames," *Journal of Structural Engineering*, (accepted).

Sorabella, S. (2006). "Ground Motion Selection for Boston, Massachusetts." *Master's Thesis.* Tufts University.